

## Desalination of Seawater from Jepara Beach uses Hollow Fiber Imprinted Membrane-Based Eugenol

Muhammad Cholid Djunaidi<sup>1\*</sup>, Nesti Dwi Maharani<sup>1</sup>, Khabibi<sup>1</sup>, Heru Susanto<sup>2</sup>, Abdullah Malik Islam Filardli<sup>2</sup>

<sup>1</sup>Department of Chemistry, Faculty of Science and Mathematics, Diponegoro University, Tembalang, Semarang 50275, Indonesia

<sup>2</sup>Department of Chemical Engineering, Faculty of Engineering, Diponegoro University, Tembalang, Semarang 50275, Indonesia

\*Corresponding author email: [choliddjunaidi@live.undip.ac.id](mailto:choliddjunaidi@live.undip.ac.id)

Received January 19, 2023; Accepted November 14, 2024; Available online March 20, 2025

**ABSTRACT.** In 2022, Indonesia will experience a major problem with clean water, almost 119 million people do not have access to clean water and are forced to consume unsuitable water. This problem is caused by poor water management and the high cost of separating using a reverse osmosis membrane. The abundance of seawater in Indonesia and Jepara in particular has encouraged researchers to create alternative desalination membranes that are efficient and selective using Hollow Fiber Desalination Imprinted Membranes (HFDIM), which are available on the market with better quality. Hollow Fiber uses an imprinted method that has good efficiency and selectivity. The variations used in this research were variations in seawater dilution concentration of 0, 3, 5, and 10 times. In tensile, biodegradable, contact angle, TGA, porosity, water absorption, flux, and transport tests, the best results were obtained using HFDIM at varying concentrations of 10 times dilution solutions with a percentage of 86.67% in the receiving phase and 10.89% in the feed phase. on HFDNIM it is 48.33% in the receiving phase and in the feed phase it is 50%.

**Keywords:** Desalination, hollow fiber, imprinted, polyeugenol

### INTRODUCTION

Indonesia in 2022 will experience a significant problem with clean water, nearly 119 million people do not have access to clean water and are forced to consume inappropriate water (Elma et al., 2020). Based on data from WHO in 2022 as many as 42% of the population will be affected by diseases caused by unsafe water, namely cholera, hepatitis, polyneuritis, dysentery trachoma to intestinal worms and diarrhea (Dewantara et al., 2018). Diarrhea accompanied by vomiting (vomiting) has symptoms of continuous bowel movements, vomiting and stomach cramps (Yeung, 2021). Clean water problems are caused by poor water management. The management system implemented so far is not under the environmental and infrastructure development which is often neglected for the conservation of water resources. Wastewater treatment and recycling plants are unimportant (Yeung, 2021). Several methods have been carried out to overcome this problem, namely desalination by separating the NaCl in seawater using multistage flash (MSF) process is a distillation method at a temperature of 90 to 110 °C but this process is expensive because it (Almerri et al., 2021). A semipermeable reverse osmosis membrane to become clean water ready for use. The membrane

must be strong, porous, not leaky, selective, not rejected by blood (hemocompatible) and able to separate NaCl in seawater (Deppisch et al., 1998; Lim et al., 2021). However, this method is very expensive and takes a long time, so it is necessary to develop better analytical methods with high sensitivity and selectivity as well as better separation and preconcentration technologies (Erna et al., 2015). One of the desalination method developments is the Molecularly Imprinted Membrane or MIM method with high selectivity because it involves molecular imprints. Molecularly Imprinted Membrane or MIM is a method or technique for making templated membranes, so they are selective for target molecules with high binding capacity and excellent permeability (Fırlak et al., 2014). In 2010, Djunaidi conducted research using polyeugenol as a functional polymer with Polyethylene Glycol Diglycidyl Ether (PEGDE) for the synthesis of MIP Fe (IIP Fe), MIP phenol, MIP vanillin and MIP Glucose (Djunaidi et al., 2010). In 2015, Djunaidi conducted further research on membrane selectivity from polyeugenol to determine the effect of adsorption on Fe(III) and Cr(III) metals in PVA solutions in NMP solvents (Djunaidi et al., 2015).

In 2018, Djunaidi researched desalination using seawater to determine the effect of salination transport

using a liquid membrane (PIM), the result is that polyeugenol can become an active compound for seawater desalination (Djunaidi, 2018). In addition, in 2020, Djunaidi researched using polyeugenol as a functional polymer with Polyethylene Glycol (PEG) 6000 and 4000 in NMP to get the best results of MIM PEG 6000 for the selective adsorption of urea. From the various problems studied regarding the matters above, it is necessary to synthesize Hollow Fiber Desalination Imprinted Membrane (HFDIM) with polyeugenol components as functional polymers with polysulfone and PEG 6000 in the form of hollow fibers, which are expected to be able to transport saline well. A comparison is made with Hollow Fiber Desalination Non-Imprinted Membrane (HFDNIM) performance.

## EXPERIMENTAL SECTION

### Instrumental

The instrumental in this research were : laboratory glassware (Pyrex and Herma), analytical balance (Mettler-200 and Ohaus), stirrer, magnetic bar, pH meter (Trans Instrument), FT-IR (Shimadzu Prestige 21) ASTM, SEM- EDX.(JEOL JSM 6510 LA), reflux apparatus; instruments for making hollow fiber; Analytical balance (Ohaus); Pestle and mortar; T3 Pots; pH paper (Macherey-Nagel); pH meter (Senz), Salinity meter (ATC), Salinity meter (KOKIDO).

### Materials

The materials in this research were : eugenol p.a. (SIGMA Aldrich),  $\text{BF}_3\text{O}(\text{C}_2\text{H}_5)_2$  (SIGMA Aldrich),  $\text{Na}_2\text{SO}_4$  technical anhydrous (Merck),  $\text{MgSO}_4 \cdot 7 \text{H}_2\text{O}$  (Merck),  $\text{Ca}(\text{OH})_2$  (Merck), NaOH p.a (Merck), methanol p.a (Merck), chloroform p.a (Merck), ethanol p.a (Merck), aquabides, polisulfon (PSF) (SIGMA Aldrich), N-Methyl 2-Pyrrolidone (NMP) (Merck), poly (ethylene glycol) 6000 (Merck).

### Procedure

#### *Polyeugenol (PE) synthesis*

5.8 g of eugenol added with 0.25 mL of  $\text{BF}_3$ -diethylether every hour. Polymerization was stopped by adding 1 mL of methanol. The gel formed was dissolved with chloroform and washed with distilled water until the pH was neutral. The solution is dried by

adding anhydrous  $\text{Na}_2\text{SO}_4$ , and evaporated at room temperature.

#### *MIM contact with template variations $\text{MgSO}_4 \cdot 7 \text{H}_2\text{O}$ and $\text{Ca}(\text{OH})_2$*

The synthesized PE is contacted with templates  $\text{MgSO}_4 \cdot 7 \text{H}_2\text{O}$  and  $\text{Ca}(\text{OH})_2$  each concentration of 1000 ppm using distilled water in a 500 mL volumetric flask. Comparison of PE: template is 1:20. It aims to include Mg and Ca molecules (templates). Then it was stirred for 24 hours and filtered and dried to form Ca-PE-Mg.

#### *Hollow Fiber Desalination Imprinted Membrane (HFDIM) based on eugenol*

Ca-PE-Mg added polysulfone and PEG 6000 in a ratio of 1:4:1 with 0.1 M NaOH catalyst 0.25 mL dissolved in 12 mL of NMP solvent stirred and refluxed for 10 hours at 90 °C. After being homogeneous or united, the dope membrane is printed using the phase inversion method on a membrane printing device. A coagulant bath filled with room temperature water is placed under the spinneret as far as 30 cm above the water's surface. The dope solution is put in tube 1 (dope tube). In tube 2, distilled water is flowed by adjusting the flowmeter. Tube 1 which contains a dope solution is connected to the compressor using a hose. Then the water tap and compressor are opened to form hollow fiber membranes. After passing through the spinneret, the dope solution enters the coagulant bath to create dense, characterized hollow fibers (Figure 1).

#### *Hollow Fiber Desalination Non Imprinted Membrane (HFDNIM) (Control)*

The synthesis of HFDNIM was carried out in the same way as the HFDIM, but the synthesized eugenol derivative was not contacted with  $\text{MgSO}_4 \cdot 7 \text{H}_2\text{O}$  and  $\text{Ca}(\text{OH})_2$  1000 ppm.

#### *Transportation by seawater from Jepara beach using HFDIM and HFDNIM*

HFDIM and HFDNIM transport membranes transport seawater from the Jepara coast using transport devices. This transport was carried out for 6 hours by taking 5 mL of samples of seawater from Jepara Beach every hour and then analyzed using a salinity meter.

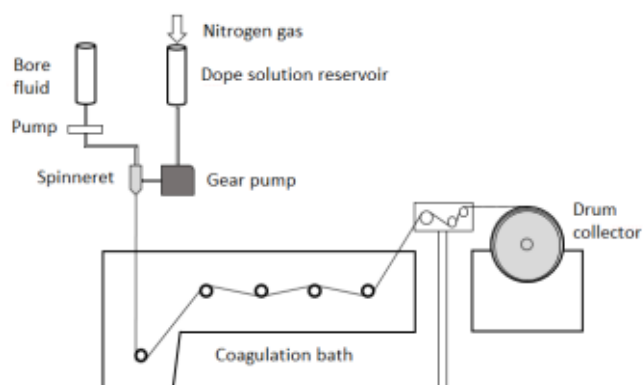


Figure 1. Hollow fiber printing equipment range (Raharjo et al., 2021)

## Characterization and Testing

### Biodegradable test

Weigh the initial weight of the membrane then place it in the fertilizer/soil and observe it every week to find out the final weight produced.

### Membrane porosity test

Soak the membrane with 10 mL of aquadamine in a petri dish for 24 hours at room temperature. Then the membrane is dried and weighed to obtain the  $W_1$  (g) value. Furthermore, the membrane was dried in an oven at 100 °C for 6 hours then cooled and weighed again so that the value of  $W_2$  (g) was obtained as the dry weight of the membrane.

### Membrane hydrophilicity test

The hydrophilicity was analyzed using the DSA (Drop Shape Analysis) method by dropping 1 drop of aquadamine right on the surface of the membrane and taking a picture with a camera angle parallel to the membrane.

### Water absorption test (Water Uptake)

The membrane was weighed to obtain the initial weight of the membrane, then immersed in 10 mL of aquadamine for 6 hours and weighed again after immersion.

## RESULTS AND DISCUSSION

### Polyeugenol (PE) Synthesis

Eugenol has 3 functional groups, namely allyl groups, hydroxy groups and methoxy groups which can be used for synthesis into polyeugenol. This allyl (propenyl) group can be polymerized cationically into a  $\beta$ -styrene group derivative. Polymerization usually uses Friedel-Craft catalysts such as  $AlCl_3$ ,  $AlBr_3$ ,  $BF_3$ -

diethyl ether,  $TiCl_4$ ,  $H_2SO_4$ , and other strong acids (Ngadiwiyana, 2005). Polymerization occurs through 3 stages which can be seen in **Figure 2**.

The initiation stage, is when the addition of  $BF_3$ -diethyl ether catalyst can accept electrons. These catalysts function as initiators in cationic processes. The allyl group of eugenol undergoes a step addition reaction, often called the cationic addition process (Ngadiwiyana, 2005; Prasetya & Sarjono, 2019). The propagation stage form covalent bonds in the cation chains from eugenol monomers, producing long monomer chains (Djunaidi & Wenten, 2019; Djunaidi, 2010). The termination stage, when the addition of methanol aims to stop the polymerization process so that the carbonium ion binds to its partner anion ( $CH_3O$  group) and the end of the polyeugenol polymer is a methoxy group (Djunaidi & Wenten, 2019; Djunaidi, 2010; Prasetya & Sarjono, 2019). The formed precipitate is dried, weighed and analyzed by FTIR. The resulting polyeugenol is in the form of an orange powder with a yield of 99%. Then FTIR analysis was carried out with the following results.

**Figure 3** shows the results of the FTIR analysis of polyeugenol, there is no spectral formation of the allyl group ( $C=C$ ) in the  $1643\text{ cm}^{-1}$  wavenumber region and vinyl groups ( $C=CH_2$ ) in the region of wavenumbers  $995$  and  $912\text{ cm}^{-1}$ . So it can be concluded that there has been a polymerization reaction. The group undergoes an addition reaction upon polymerization as described by (Djunaidi & Wenten, 2019; Djunaidi, 2010), that the polymerization reaction can be an addition reaction. Thus, the process of making polyeugenol was successfully carried out.

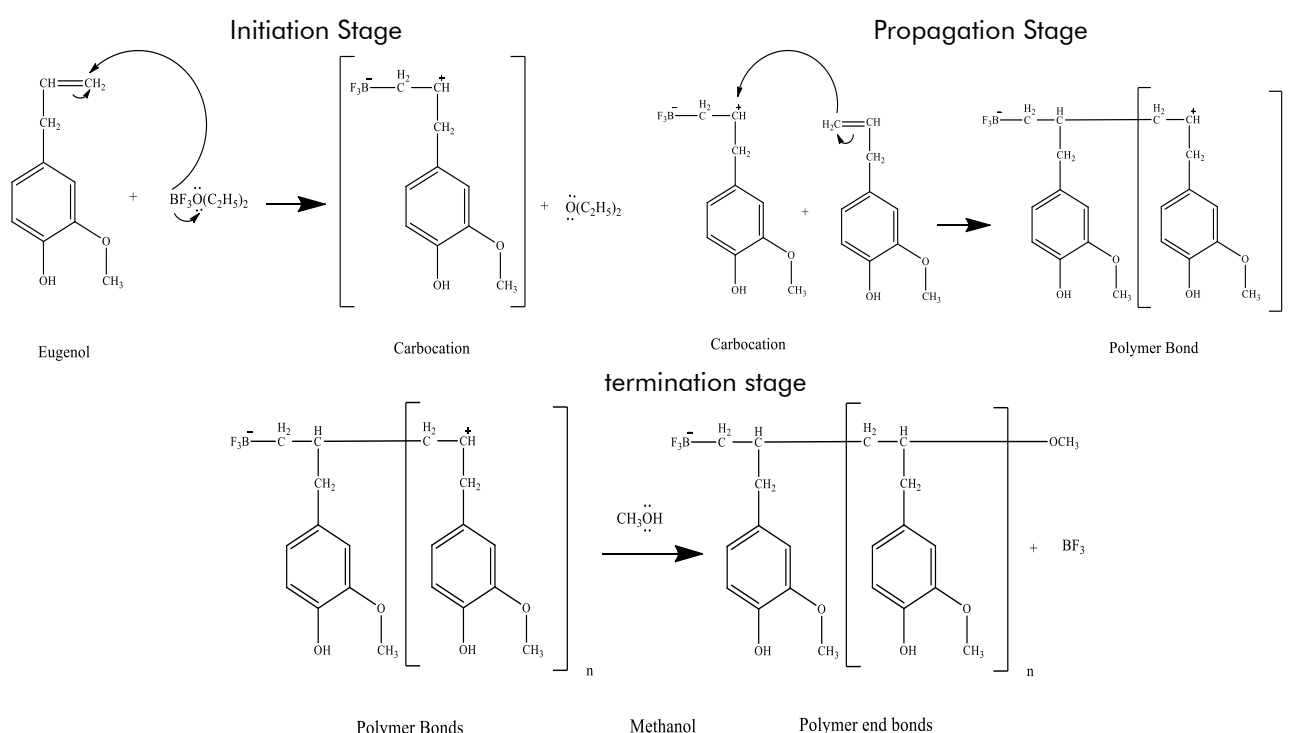


**Figure 2.** Mechanism of polyeugenol polymerization of eugenol (Djunaidi, 2010)

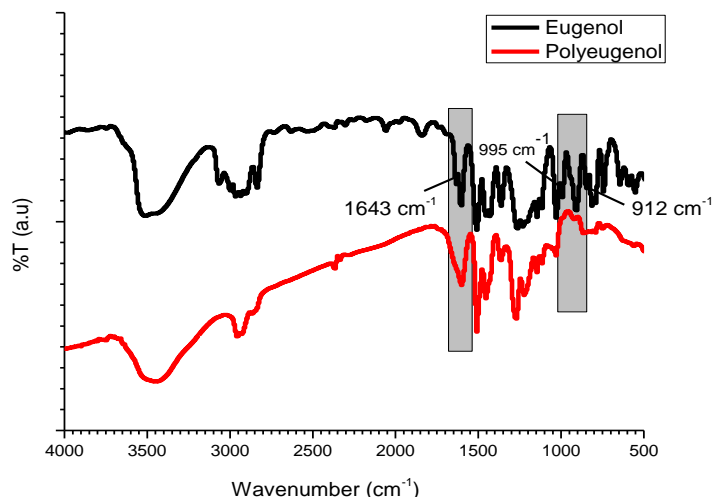


Figure 3. FTIR Comparison results of eugenol and polyeugenol

Table 1. Mg(II)-PE-Ca(II) contact result data

Imprinted with Polyeugenol	Before Contact (ppt)	Mixed Solution during 1 hour (ppt)	After Contact Of 24 hours (ppt)	Adsorbed Concentration (ppt)
Ca(OH) <sub>2</sub> (ppt)	9.2	17	2	15
Mg(SO <sub>4</sub> ). 7 H <sub>2</sub> O (ppt)	8.0			

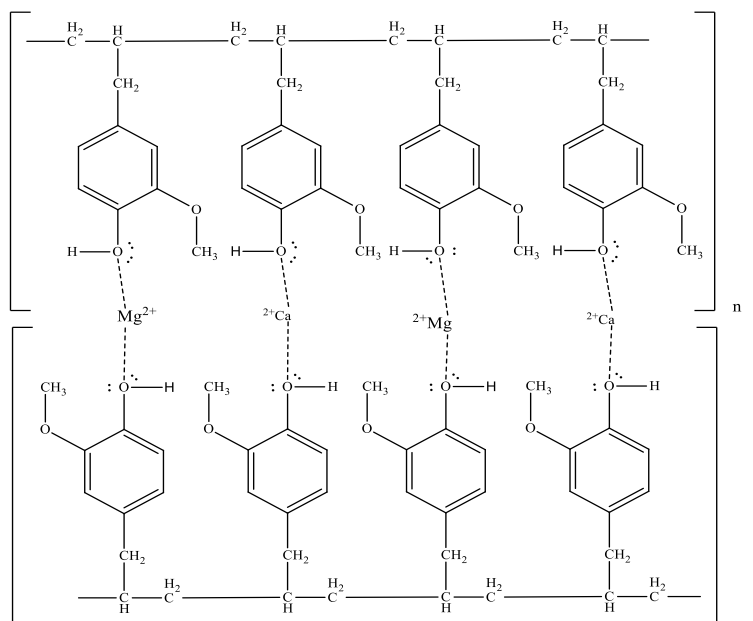


Figure 4. Possible interactions that occur between Polyeugenol with Mg(II) and Ca(II)

**Contact with Solution MgSO<sub>4</sub> .7 H<sub>2</sub>O and Ca(OH)<sub>2</sub>**

The Ca and Mg metals used for contacting are Ca(OH)<sub>2</sub> solutions and MgSO<sub>4</sub>.7H<sub>2</sub>O during 24 hours with a concentration of about 1000 ppm each. The test results using a Salinity meter were obtained for the contacted Mg(II)-PE-Ca(II), which can be seen in Table 1. Table 1 shows that the metal contacted on the polymer reaches 88.24% with a concentration of 15 ppt. This is due to the non-covalent interactions that occur in the printing process with polyeugenol because

the interactions that occur have relatively weak bonds such as hydrogen bonds. The possible reactions are shown in the Figure 4 (Djunaidi & Wenten, 2019; Ziegenheim et al., 2020).

The FTIR results show a comparative analysis as shown in Figure 5. Figure 5 shows absorption bands of hydroxyl groups (-OH) at wavenumber 3400 cm<sup>-1</sup>, S=O groups at wavenumber 1013 cm<sup>-1</sup>, SO groups at wavenumber 1237 cm<sup>-1</sup> and C-S groups at wavenumber waves 694 cm<sup>-1</sup>. The absorption band of

the O-Ca and O-Mg group at the PE-D wavenumber is  $756\text{ cm}^{-1}$ . The absorption band of the hydroxyl group (-OH) on PE-D has a greater intensity than Polyuegenol, this is due to the role of metal ions Mg(II) and Ca(II) which have been templated in polyuegenol. Whereas in HFDIM and HFDNIM the intensity of the -OH group is reduced because the template has been released when the phase inversion of the membrane occurs (making a hollow) (Djunaidi et al., 2024;

Ziegenheim et al., 2020). Estimated interactions occurring polyuegenol contact glucose, polysulfone and PEG 6000 can be shown in **Figure 6**.

SEM results show the effect of imprinted Mg(II) and Ca(II) on membrane morphology using a magnification of 3000 times. The cross-section of the membrane uses a magnification of 60 times as shown in **Figure 7**.

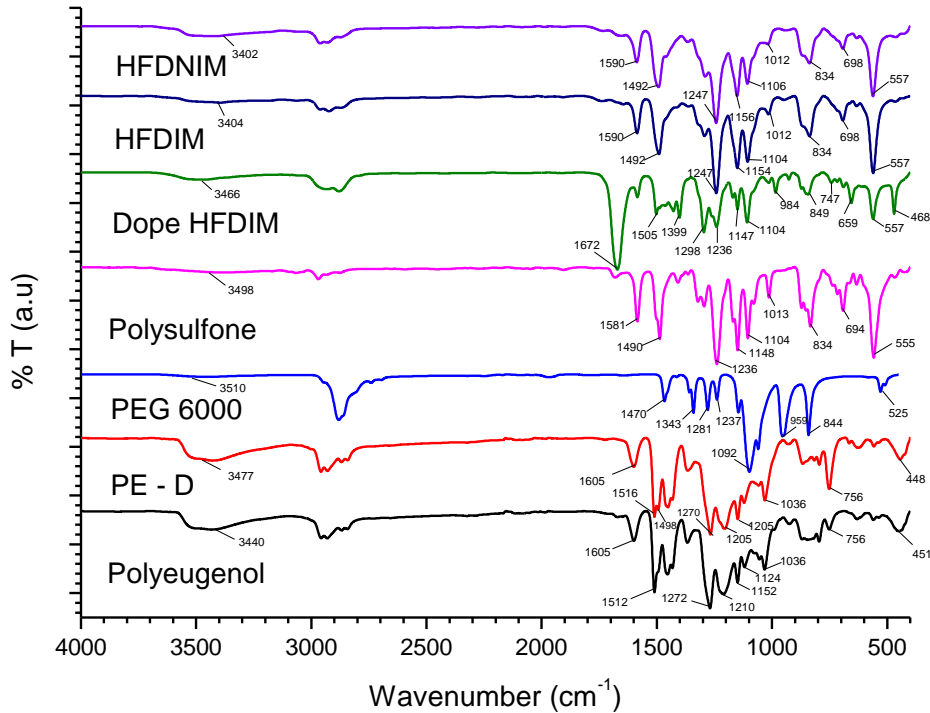


**Figure 5.** Comparison results of FTIR polyuegenol, PEG 6000, polysulfone, HFDIM and HFDNIM

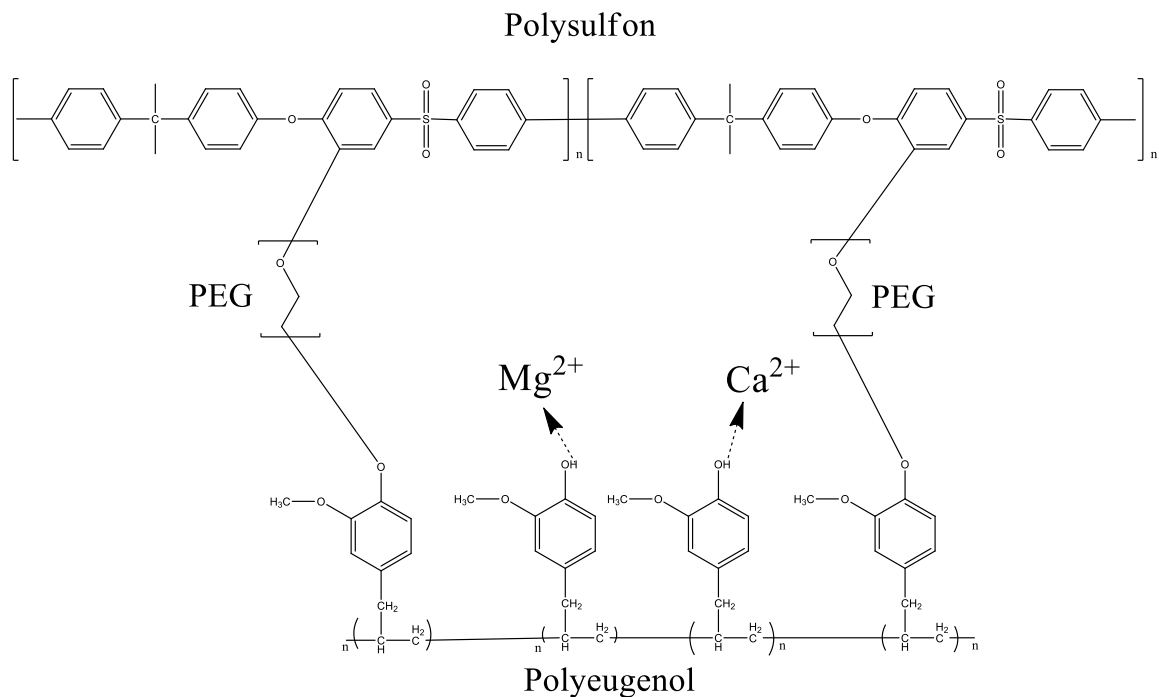


**Figure 6.** Estimated interactions occurring polyuegenol contact glucose, polysulfone and PEG 6000

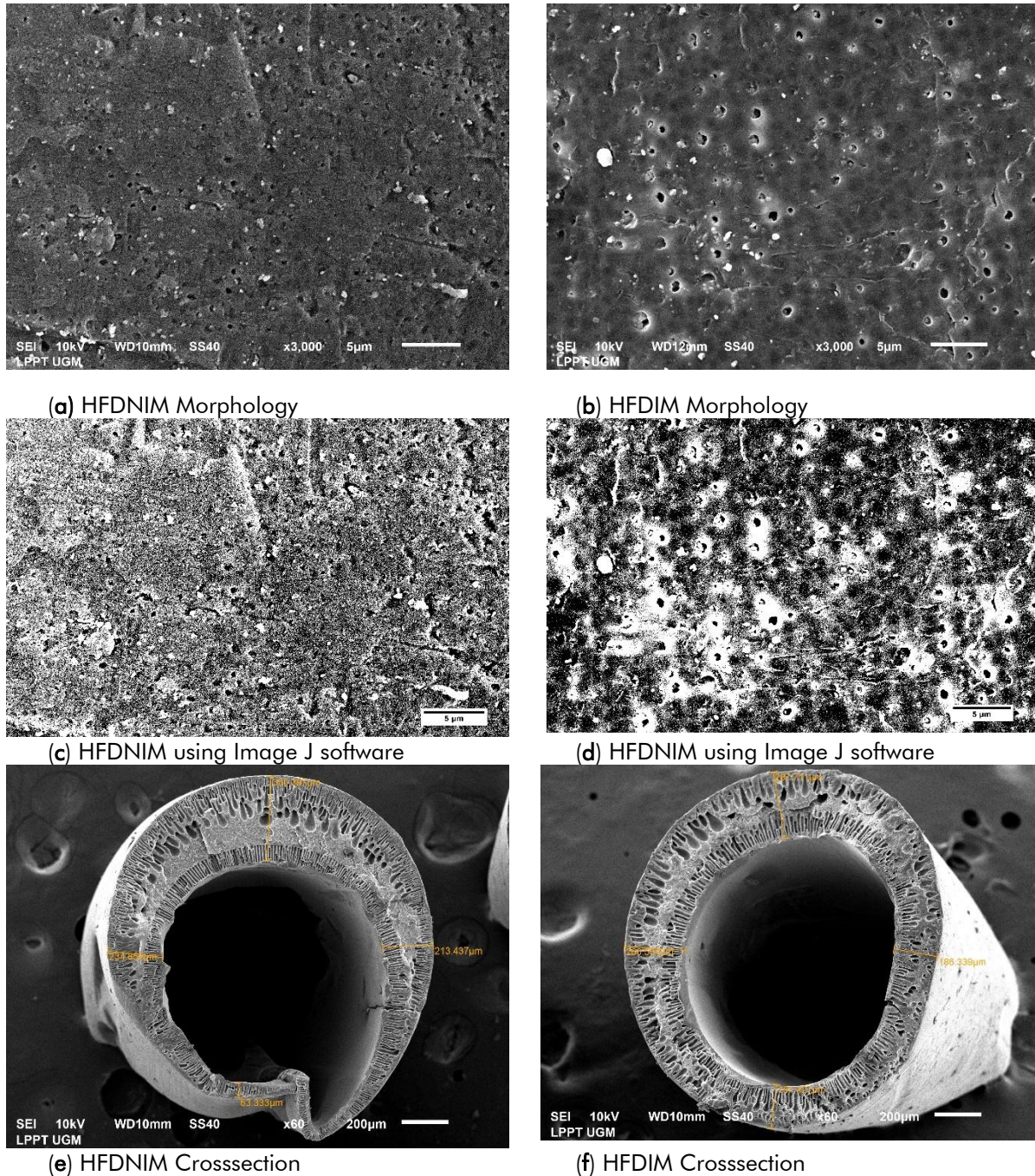


**Figure 7.** Membrane SEM results in (a) Morphology of HFDNIM, (b) Morphology of HFDIM, (c) Morphology of HFDNIM with Image J software, (d) Morphology of HFDIM with Image J software, (e) Cross section of HFDNIM, (f) Cross section of HFDIM

**Table 2.** Comparison of Pore Size Between HFDIM and HFDNIM Membranes with Image J software

	HFDIM	HFDNIM
Counted number of pores	259687	173395
Total Areas	159.011	78.608
% Area	36.314	14.483

Figure 7 and Table 2 show the results of surface morphology and cross-section using SEM, it can be seen that the morphology of the HFDIM membrane has pores that are not uniform in size compared to

HFDNIM in the form of composite asymmetry. A cross-section of the HFDIM membrane forms a finger-like macrovoid compared to the HFDNIM image (Khoiroh et al., 2019; Maggay et al., 2022; Verma et al.,

2018). This is because when the hollow fibre membrane after being printed is then immersed in a coagulation bath containing aquabides the membrane will precipitate and the formation of membrane pores occurs due to the weak solubility of the three materials in water causing the exchange of NMP solvents with water much more quickly to form macrovoid finger-like (finger).

**Biodegradable Test on HFDIM and HFDNIM**

Figure 8 shows the results of the biodegradable test on HFDIM and HFDNIM as shown below. Figure 8 shows the results of biodegradable measurements on HFDIM and HFDNIM which aim to determine how long the membrane constituent material can be thoroughly degraded. The faster the membrane mass decreases, the better the membrane material decomposes quickly and is safe for the environment. The results of biodegradable membranes can be shown as shown in Figure 8. Figure 8 shows the percentage of biodegradable in HFDIM which has a

biodegradable percentage of 18% and HFDNIM has a biodegradable percentage of 23.4%. This is due to the addition of Ca(II) and Mg(II) templates with hydrophilic OH groups so that more water molecules are absorbed into the membrane’s pores, making it easier for microorganisms to decompose (Brown et al., 2018).

**Tensile Test on HFDIM and HFDNIM**

Figure 9 shows the tensile test results on HFDIM and HFDNIM, as shown below. Figure 9 shows the results of tensile test measurements on HFDIM and HFDNIM which aims to determine the strength of the membrane constituent material (mechanical properties of the membrane) which can be seen from the value of Young's modulus. The greater Young's modulus value, the better the membrane material decomposes quickly and is environmentally safe. The results of the membrane tensile test can be shown as shown in Figure 9.

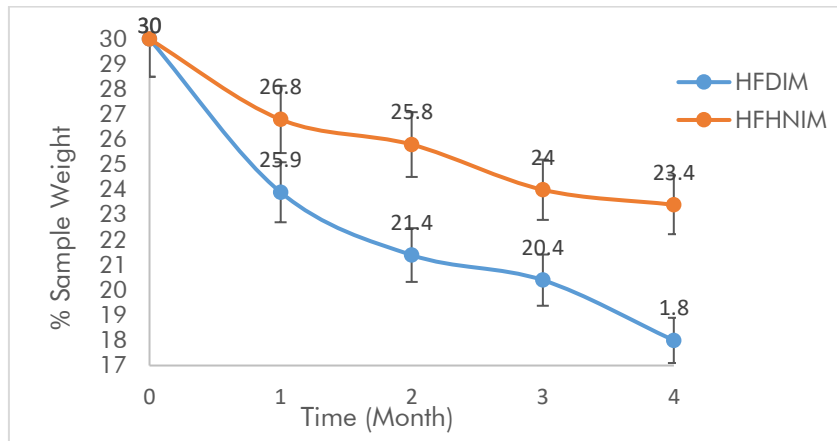


Figure 8. Graph of biodegradable membrane results: (a) HFDIM (b) HFDNIM

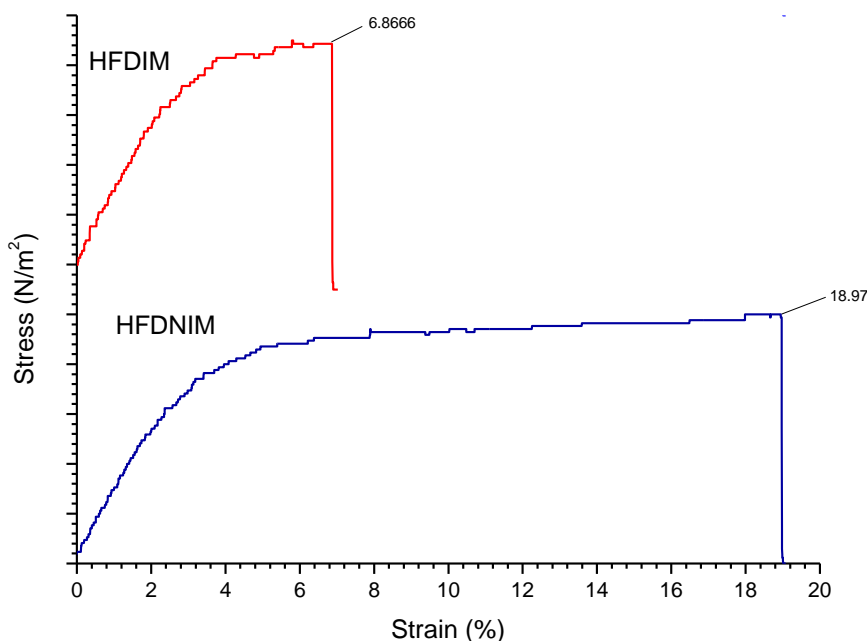


Figure 9. Graph of membrane tensile test results: (a) HFDIM (b) HFDNIM

**Table 3.** Comparison of Young's modulus values between HFDIM and HFDNIM membranes

Membranes variation	Strains (%)	Stress (N/M <sup>2</sup> )	Young's modulus (N/M <sup>2</sup> )
HFDIM	6.8666	2.0859	0.3038
HFDNIM	18.97	0.9882	0.0521

**Figure 9** shows the percentage of biodegradable in HFDIM has a Young's modulus value of 0.3038 N/M<sup>2</sup> and HFDNIM has a biodegradable percentage of 0.0521 N/M<sup>2</sup>. This is due to adding of a salt template with hydrophilic OH groups so that strength is needed to destroy the membrane (Brown et al., 2018). The increase in the tensile test is directly proportional to the results of the biodegradable test.

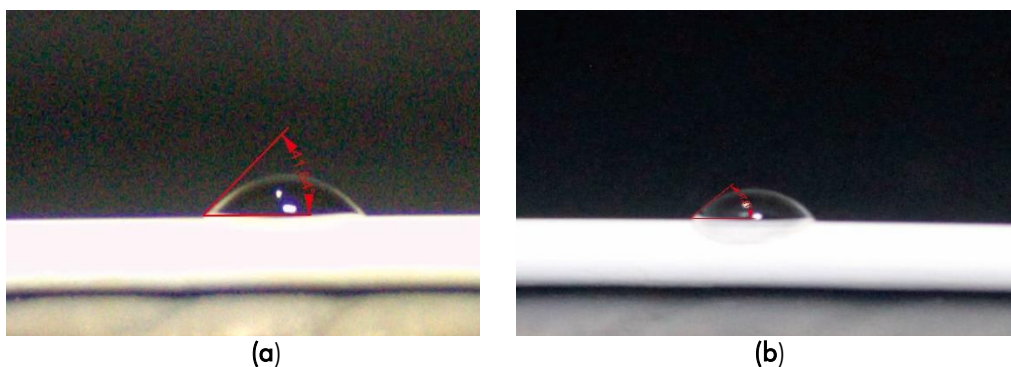
**Contact Angle Test on HFDIM and HFDNIM**

Figure 10 shows the results of the Membrane Contact Angle due to the influence of Ca(II) and Mg(II) metal imprints on HFDIM and HFDNIM as shown in Figure 10 below. Figure 10 shows the results of measuring the contact angle using the DSA (Drop Shape Analysis) method on HFDIM and HFDNIM which aims to determine the interactions between the membrane and water molecules if the membrane is hydrophobic then the value of the membrane contact angle is more than 90 ° while if the membrane is hydrophilic then the value of the contact angle is less than 90 ° (Djunaidi et al., 2020). The results of the contact angle show a comparative analysis as shown in **Figure 10**. **Figure 10** shows the results of the contact

angle on HFDIM which has an angle of 41.64 ° and HFDNIM's biodegradation percentage of 47.21 °. This is due to the addition of Ca(II) and Mg(II) templates which have hydrophilic OH groups so that more water molecules are absorbed into the pores in the membrane because they can form physical interactions such as intermolecular hydrogen bonds between the functional groups of membrane compounds (OH) and water that is able to pass through the pores outside the membrane. It can be concluded that only the printed metal which dissolves in water is absorbed in HFDIM so that other metals will be retained and cannot enter the membrane.

**TGA test on HFDIM and HFDNIM**

**Figure 11** shows the tensile test results on HFDIM and HFDNIM as shown below. It shows the results of the TGA test measurements on HFDIM and HFDNIM which aims to determine the level of membrane stability which varies with the influence of temperature. The greater the % mass loss, the better the membrane material decomposes quickly and is safe for the environment. The results of the TGA membrane test can be shown as shown in **Figure 11**.



**Figure 10.** Results of membrane contact angle (a) HFDIM, (b) HFDNIM

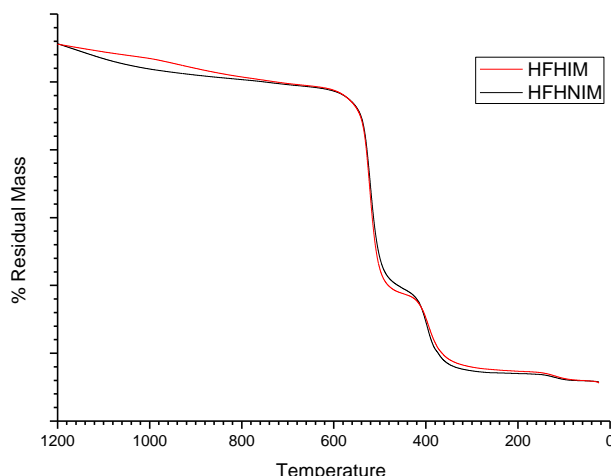


**Figure 11.** Results of TGA membrane analysis (a) HFDIM, (b) HFDNIM

**Figure 11** shows the results of TGA analysis using the thermal analysis method on variations of HFDIM and HFDNIM, which aims to determine the level of membrane stability which varies with the influence of temperature. The decrease in the mass of HFDIM  $T_{1-5\%}$  occurred in the temperature range of 92.18 - 334.17 °C and the reduction in the mass of HFDIM  $T_{1-5\%}$  occurred in the temperature range of 110.73 - 355.75 °C. The addition of Ca(II) and Mg(II) templates on the thermal stability of the membrane cannot be maintained (thermodynamically less stable), so the results show a decrease in the decomposition temperature of the membrane material (Guillen et al., 2011). It can be concluded that the addition of a template has a lower degradation temperature (easier to be degraded by temperature) which has the potential to disrupt polymer chains, especially hydrogen bonds, so they tend to be unstable and more brittle.

#### Porosity Test on HFDIM and HFDNIM

**Figure 12** shows the results of porosity measurements on HFDIM and HFDNIM which aims to determine the number of interactions between the membrane and water molecules (how much the membrane can adsorb). The higher the porosity of the membrane, the more space (macrovoid) in the

membrane. The results of membrane porosity can be shown as shown in **Figure 12**. **Figure 12** shows the results of the porosity test analysis for HFDIM having a porosity percentage of 90.01% and HFDNIM having a porosity percentage of 69.69%. This is due to the addition of Ca(II) and Mg(II) templates which have hydrophilic OH groups so that more water molecules are absorbed into the membrane pores because they can form physical interactions such as intermolecular hydrogen bonds between the functional groups of membrane constituent compounds (OH) and water capable of passing through the pores of the membrane.

#### Water Absorption Test on HFDIM and HFDNIM

**Figure 13** shows the results of the water absorption test due to the influence of Ca(II) and Mg(II) moulds on HFDIM and HFDNIM. **Figure 13** shows the results of measuring water absorption in HFDIM and HFDNIM which aims to determine the ability of the membrane to absorb water (the number of empty membrane cavities that interact with water). The higher the water absorption of the membrane, the more space (macrovoid) in the membrane (Djunaidi et al., 2020; Jalali et al., 2016). The results of membrane porosity can be shown as shown in **Figure 13**.

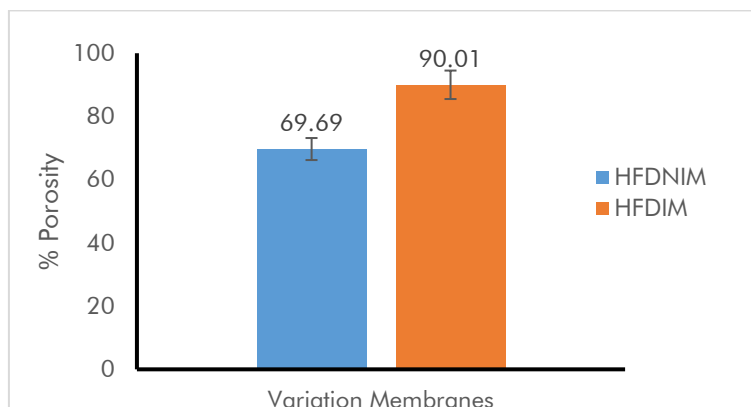


**Figure 12.** Graph of membrane porosity results: (a) HFDIM (b) HFDNIM

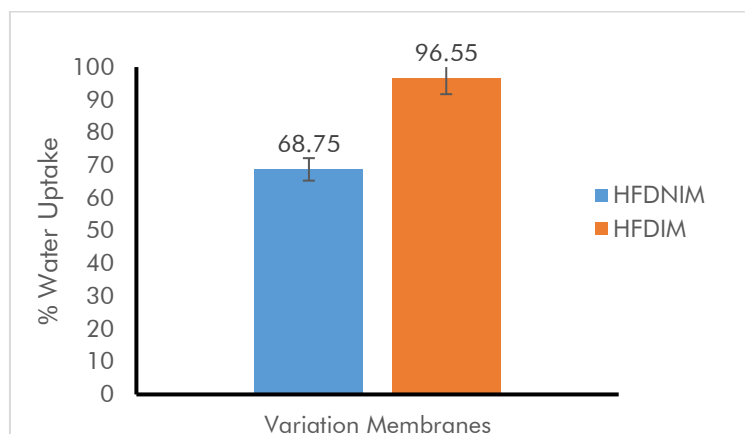


**Figure 13.** Graph of membrane water absorption results: (a) HFDIM (b) HFDNIM

**Figure 13** shows the results of the water absorption analysis of HFDIM has a percentage of 90.01% and HFDNIM having a percentage of 69.69%. This is due to the addition of Ca(II) and Mg(II) templates which have hydrophilic OH groups so that more water molecules are absorbed into the membrane pores because they can form physical interactions such as intermolecular hydrogen bonds between the functional groups of membrane constituent compounds (OH) and water. Capable of passing through the pores of the membrane. The increase in the water absorption test is directly proportional to the results of the porosity, biodegradable, tensile and TGA tests.

**Flux Test Using HFDIM and HFDNIM with Seawater Dilution Variations**

**Figure 14** shows the results of the flux test due to the influence of Ca(II) and Mg(II) moulds that the results of flux measurements on HFDIM and HFDNIM which aim to determine the size of the pores in the membrane using various types of solutions containing different molecular weights. If the value of the membrane flux is higher, the pores in the membrane (macrovoid) can be passed through the solution (Lim et al., 2021). The results of membrane flux can be shown as shown in **Figure 14**. **Figure 14** shows that HFDIM has a percentage value of water flux of 843.47 L/m<sup>2</sup> hours and seawater of 726.11 L/m<sup>2</sup> hours.

HFDNIM has a water flux value of 614.97 L/m<sup>2</sup> hours and seawater of 510.67 L/m<sup>2</sup> hours. This can happen because HFDIM has a Ca(II) template measuring 9.9 nm and Mg(II) measuring 6.6 nm which is capable of pushing anions smaller in size than Mg(II) in seawater (Djunaidi & Wenten, 2019; Raharjo et al., 2019). HFDIM have high affinity Mg(II). Therefore, the polymer exhibits a selectivity separation factor greater (Jamoussi et al., 2023).

**Sea Water Transport with Dilution Variations 0, 3, 5 and 10 times using HFDIM and HFDNIM**

Seawater transport uses 4 dilution variations, namely 0, 3, 5, and 10 times aiming to determine the optimum seawater concentration with maximum transport results in HFDIM and HFDNIM using dilution variations. The results of the transport can be seen in **Figure 15**. **Figure 15** shows the results of seawater transport with a variation of 0 times dilution that the percentage of seawater transport in HFDIM is 44.74% in the receiving phase and the remaining in the feed phase is 51.80%. Whereas in HFDNIM it is 15.15% in the receiving phase and the remaining in the feed phase is 81.82%. In the variation of 3 times dilution, the percentage of seawater transport in HFDIM was 67.30% in the receiving phase and 29.52% in the feed phase. Whereas in HFDNIM it is 24.18% in the receiving phase and the remaining in the feed phase is 73.63%. In the 5 times dilution variation,

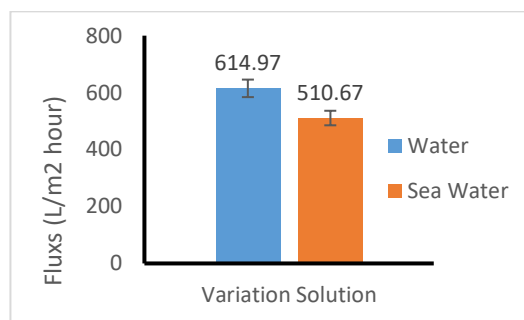
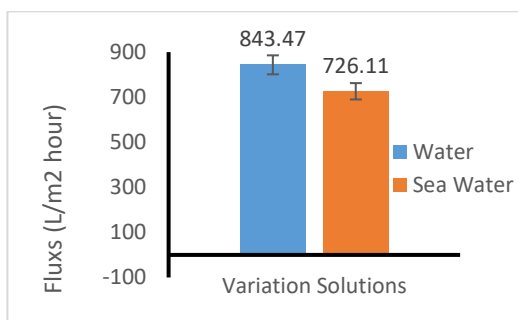
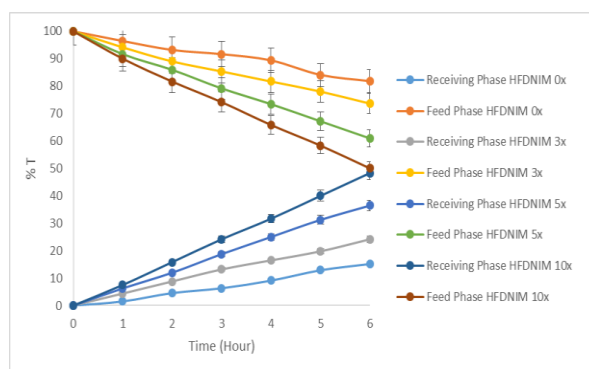
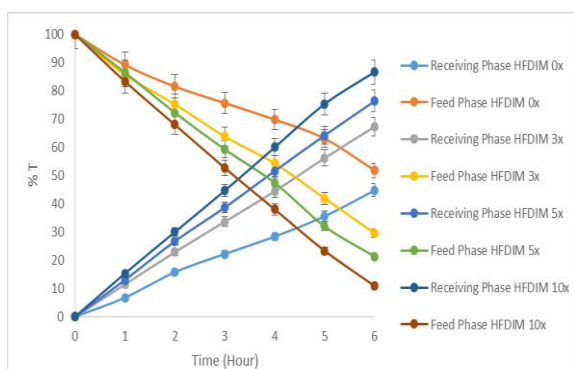


**Figure 14.** Graph of membrane flux results: (a) HFDIM (b) HFDNIM



**a) HFDIM** **b) HFDNIM**

**Figure 15.** Graph of percentage of seawater transport results with variations of dilution solutions 0, 3, 5, 10 times on a) HFDIM and b) HFDNIM

the percentage of seawater transport in HFDIM was 76.36% in the receiving phase and 21.33% in the feed phase. In HFDNIM it is 36.46% in the receiving phase and the remaining in the feed phase 60.94%. In the 10 times dilution variation, the percentage of urea transport in HFDIM was 86.67% in the receiving phase and 10.89% remaining in the feed phase. Whereas in HFDNIM it is 48.33% in the receiving phase and the remaining in the feed phase is 50%. This can happen because HFDIM has a Ca(II) template and Mg(II) is a metal cation. Metal ions Ca(II) measuring 9.9 nm and Mg(II) measuring 6.6 nm are capable of pushing anions smaller than Mg(II) in seawater to move from the feed phase to the receiving phase. Thus the transport of HFDIM is much larger than that of HFDNIM 33% in the receiving phase and the remaining 50% in the feed phase. This can happen because HFDIM has a Ca(II) template and Mg(II) is a metal cation. Metal ions Ca(II) measuring 9.9 nm and Mg(II) measuring 6.6 nm are capable of pushing anions smaller than Mg(II) in seawater to move from the feed phase to the receiving phase. Thus the transport of HFDIM is much larger than that of HFDNIM 33% in the receiving phase and the remaining 50% in the feed phase. This can happen because HFDIM has a Ca(II) template and Mg(II) is a metal cation. Metal ions Ca(II) measuring 9.9 nm and Mg(II) measuring 6.6 nm are capable of pushing anions smaller than Mg(II) in seawater to move from the feed phase to the receiving phase. Thus the transport of HFDIM is much larger than that of HFDNIM (Dewantara et al., 2018; Djunaidi, 2018; Raharjo et al., 2021).

## CONCLUSIONS

Desalination of Jepara Beach Seawater using the Ca(II) and Mg(II) imprint method in the form of hollow fiber (HFDIM) has a pore number of 259687 so that the porosity value is 90.01%, water absorption is 90.01%, flux is 726.11 L/m<sup>2</sup>, 18% biodegradable, Young's modulus value of 0.3038 N/m<sup>2</sup> and membrane hydrophilicity of 41.64 $\mu$  and begins to decompose at a temperature of 92.18 – 334.17 °C. This causes the results of the transport HFDIM with dilution 10 times better than HFDNIM.

## ACKNOWLEDGEMENTS

The author would like to thank Diponegoro University for the research project entitled DESALINATION OF SEAWATER FROM JEPARA BEACH USES HOLLOW FIBRE IMPRINTED MEMBRANE-BASED EUGENOL. Based on the assignment letter Directorate of Research and Community Service Deputy for Strengthening Research and Development Ministry of Research and Technology / National Research and Innovation Agency SPK Number : 753-23 / UN7.D2 / PP / IX / 2022

## REFERENCES

- Almerri, A. H., Al-Obaidi, M. A., Alsadaie, S., & Mujtaba, I. M. (2021). Modelling and simulation of industrial multistage flash desalination process with exergetic and thermodynamic analysis. A case study of Azzour seawater desalination plant. *Chemical Product and Process Modeling*, 18(1), 73-95.
- Brown, D. M., Hughes, C. B., Spence, M., Bonte, M., & Whale, G. (2018). Assessing the suitability of a manometric test system for determining the biodegradability of volatile hydrocarbons. *Chemosphere*, 195, 381-389.
- Deppisch, R., Storr, M., Buck, R., & Göhl, H. (1998). Blood material interactions at the surfaces of membranes in medical applications. *Separation and purification technology*, 14(1-3), 241-254.
- Dewantara, I. G. Y., Suyitno, B. M., & Lesmana, I. G. E. (2018). Desalinasi air laut berbasis energi surya sebagai alternatif penyediaan air bersih (Solar energy-based seawater desalination as an alternative for providing clean water). *Jurnal Teknik Mesin (JTM)*, 7(1), 1-4.
- Djunaidi, M., Pardoyo, P., & Wahyuni, T. (2020). Influence of different carriers in polymer Inclusion Membranes for Desalination of Seawater. *Asian Journal of Chemistry*, 32, 1869-1873. doi:10.14233/ajchem.2020.22636
- Djunaidi, M., & Wenten, I. G. (2019). Synthesis of eugenol-based selective membrane for hemodialysis. *IOP Conference Series: Materials Science and Engineering*, 509, 012069. doi:10.1088/1757-899X/509/1/012069
- Djunaidi, M. C., Lusiana, R.A., & Kartikawati, N.G. (2010). Sintesis polieugenol dengan katalis BF3 dietil eter untuk ekstraktan logam berat (Synthesis of polyeugenol with BF3 diethyl ether catalyst for heavy metal extractants). *Prosiding Seminar Nasional Kimia dan Pendidikan Kimia*.
- Djunaidi, M. C., Jumina, J., Ulbricht, M. (2015). Synthesis of Fe (III) Ionic Imprinted imprinted polyeugenol using polyethylene glycol diglycidylether as cross-linking agent for sorption of Fe (III). *Indonesian Journal of Chemistry*, 15(3), 305-314. <https://doi.org/10.22146/ijc.21200>.
- Djunaidi, M. C., Fauzi, H. & Hastuti, R. (2018). *Desalination of sea water using polymer inclusion membran (PIM) with aliquat 336-TBP (Tributyl Phosphate) as carrier compound*. paper presented at the matec web series 156 (2018) The 24th Regional Symposium on Chemical Engineering (RSCE 2017).
- Djunaidi, M. C., Lusiana, R. A., Wibawa, P. J., Siswanta, D., & Jumina, J. (2010). Sintesis turunan polieugenol sebagai carrier bagi recovery logam berat dengan teknik membran cair (Synthesis of polyeugenol derivatives as

- carriers for heavy metal recovery using liquid membrane techniques). *2010*, 8. doi:10.14710/reaktor.13.1.16-23
- Djunaidi, M. C., Maharani, N. D., Pardoyo, P., & Raharjo, Y. (2024). Hollow fiber hemodialysis imprinted membrane based on eugenol for human blood filter. *Indonesian Journal of Chemistry*, *24*(5), 1253-1267.
- Djunaidi, M. C., Prasetya, N. B. A., Khoiriyah, A., Pardoyo, P., Haris, A., & Febriola, N. A. (2020). Polysulfone influence on au selective adsorbent imprinted membrane synthesis with sulfonated polyeugenol as functional polymer. *Membranes*, *10*(12), 390.
- Elma, M., Mahmud, M., Akhbar, A., Suryani, L., Mustalifah, F. R., Rahma, A., . . . Baity, N. (2020). Aplikasi membran silika-pektin untuk desalinasi air payau. *Jukung (Jurnal Teknik Lingkungan)*, *6*(1).
- Erna, M., Haryati, S., Naldo, R., & Yana, Y. F. (2015). Ketahanan membran komposit kitosan/polisulfon terhadap pH (Resistance of chitosan/polysulfone composite membrane to pH.). *Jurnal Riset Kimia*, *2*(1), 29.
- Fırlak, M., Yetimoğlu, E. K., & Kahraman, M. V. (2014). Adsorption of Au (III) ions from aqueous solutions by thiol-ene photoclick hydrogels and its application to electronic waste and geothermal water. *Journal of Water Process Engineering*, *3*, 105-116.
- Guillen, G. R., Pan, Y., Li, M., & Hoek, E. M. (2011). Preparation and characterization of membranes formed by nonsolvent induced phase separation: a review. *Industrial & Engineering Chemistry Research*, *50*(7), 3798-3817.
- Jalali, A., Shokravi, A., Vatanpour, V., & Hajibeygi, M. (2016). Preparation and characterization of novel microporous ultrafiltration PES membranes using synthesized hydrophilic polysulfide-amide copolymer as an additive in the casting solution. *Microporous and Mesoporous Materials*, *228*, 1-13.
- Jamoussi, B., Chakroun, R., Al-Mur, B. A., Halawani, R. F., Aloufi, F. A., Chaabani, A., & Aljohani, N. S. (2023). Design of a new phthalocyanine-based ion-imprinted polymer for selective lithium recovery from desalination plant reverse osmosis waste. *Polymers*, *15*(18), 3847.
- Khoiroh, N., Utomo, W. P., & Fansuri, H. (2019). Fabrikasi membran asimetris LaO, 7SrO, 3CoO, 2FeO, 8O3-δ (LSCF 7328) dengan penambahan aditif polietilen glikol (PEG) (Fabrication of asymmetric membrane LaO, 7SrO, 3CoO, 2FeO, 8O3-δ (LSCF 7328) with the addition of polyethylene glycol (PEG) additives). *Jurnal Sains dan Seni ITS*, *7*(2), 30-35.
- Lim, Y. J., Goh, K., Kurihara, M., & Wang, R. (2021). Seawater desalination by reverse osmosis: Current development and future challenges in membrane fabrication—A review. *Journal of Membrane Science*, *629*, 119292.
- Maggay, I. V., Yu, M.-L., Wang, D.-M., Chiang, C.-H., Chang, Y., & Venault, A. (2022). Strategy to prepare skin-free and macrovoid-free polysulfone membranes via the NIPS process. *Journal of Membrane Science*, *655*, 120597.
- Ngadiwiyana, N. (2005). Polimerisasi eugenol dengan katalis asam sulfat pekat (Polymerization of eugenol with concentrated sulfuric acid catalyst). *Jurnal Kimia Sains dan Aplikasi*, *8*(2), 43-47.
- Prasetya, N. B. A., & Sarjono, P. R. (2019). Synthesis of copolymer eugenol crosslinked with divinyl benzene and preliminary study on its antibacterial activity. Paper presented at the *IOP Conference Series: Materials Science and Engineering*.
- Raharjo, Y., Fahmi, M.Z., Wafiroh, S., Widati, A.A., Amanda, E.R., Ismail, A.F., Othman, M.H.D., & Santoso, D. (2019). Incorporation of imprinted-zeolite to polyethersulfone/cellulose acetate membrane for creatinine removal in hemodialysis treatment. *Jurnal Teknologi*, *81*(3).
- Raharjo, Y., Ismail, A. F., Othman, M. H. D., Rosid, S. M., Azali, M. A., & Santoso, D. (2021). Effect of polymer loading on membrane properties and uremic toxins removal for hemodialysis application. *Journal of Membrane Science and Research*, *7*(1), 14-19.
- Verma, S. K., Modi, A., Singh, A. K., Teotia, R., & Bellare, J. (2018). Improved hemodialysis with hemocompatible polyethersulfone hollow fiber membranes: In vitro performance. *Journal of Biomedical Materials Research Part B: Applied Biomaterials*, *106*(3), 1286-1298.
- Yeung, S.-C. J. (2021). Diarrhea. In *oncologic emergency medicine: Principles and practice* (pp. 357-365): Springer.
- Ziegenheim, S., Szabados, M., Kónya, Z., Kukovecz, Á., Pálkó, I., & Sipos, P. (2020). Differential precipitation of Mg (OH) 2 from CaSO4· 2H2O using citrate as inhibitor—A promising concept for reagent recovery from MgSO4 waste streams. *Molecules*, *25*(21), 5012.